Density dependence of nonresonant tunneling in asymmetric coupled quantum wells

D. H. Levi,* D. R. Wake, and M. V. Klein
Materials Research Laboratory and Department of Physics, University of Illinois at Urbana-Champaign, Urbana, Illinois 61801

S. Kumar and H. Morkoç
Coordinated Science Laboratory, University of Illinois at Urbana-Champaign, Urbana, Illinois 61801
(Received 20 March 1991; revised manuscript received 11 October 1991)

We have measured tunneling rates in a series of asymmetric coupled quantum wells as a function of the barrier thickness and carrier density between confined levels in which optical-phonon-assisted tunneling is energetically forbidden. Our measurements have demonstrated a strong density dependence of the tunneling rates. The measured dependence is qualitatively consistent with a model of excitons diffusing to a limited number of extrinsic tunneling sites.

The fundamental quantum-mechanical process of tunneling is presently an area of intense investigation in semiconductor heterostructures. The initial proposal of semiconductor superlattices by Esaki and Tsu[1,2] was in part motivated by the possibility of obtaining negative differential resistance due to electron tunneling. Since that original proposal there have been many studies of tunneling in semiconductor heterostructures, initially focusing primarily on transport measurements.[3] More recently optical techniques have been applied to gain direct knowledge of the interactions mediating the tunneling process.[4–17] Most optical studies have focused on resonance conditions and the electric-field dependence of tunneling rates. In this study we focus on the carrier concentration and barrier width dependence of nonresonant tunneling rates in samples with a band structure such that LO-phonon emission is not energetically available during tunneling. As expected there is an exponential dependence of tunneling rate on barrier width. A more surprising result is a strong density dependence of these rates which is independent of barrier width. The nature of the density dependence and its invariance with barrier thickness indicates that the dominant mechanism responsible for the nonresonant tunneling process in these samples is an extrinsic effect, most likely scattering or trapping at impurities localized at the quantum-well interface.

To gain some insight into such nonresonant tunneling processes we have measured tunneling rates of band-edge carriers between lowest energy conduction subbands in adjacent wells with an energy separation of 11 meV. The structures studied are MBE-grown, nominally undoped multiple quantum wells consisting of coupled GaAs quantum wells of nominal widths of 135 and 200 Å separated by $Al_{0.35}Ga_{0.65}As$ barriers of 40, 35, 30, and 20 Å. A sample with barrier width 300 Å has been designed as a "control" sample, i.e., tunneling is not expected to occur for barriers of this thickness. Each sample consists of 15 periods of these coupled wells separated by $Al_{0.35}Ga_{0.65}As$ barriers of 350 Å between periods. We used a picosecond pump and probe transmission technique to measure carrier lifetimes in these structures both as a function of barrier width between wells, and photoexcited carrier density. Independently tunable pulses were generated by two Styryl-8 dye lasers that were synchronously pumped by a mode-locked argon-ion laser. Temporal resolution was pulse-width limited at 5 ps, while spectral resolution was limited by the 1-meV linewidth of the lasers. In these experiments the energy of an intense pump pulse is tuned in resonance with the $n=1$ heavy-hole exciton in the narrow well, thereby exciting approximately equal densities of carriers in both wells. A weaker probe pulse in resonance with the $n=1$ excitonic transition is then used to measure the decay of the carrier populations in either the narrow or wide well. The pump and probe lasers were cross polarized; the pump was focused to an ~ 50-μm spot while the probe was focused to ~ 30 μm. The probe was chopped at 4 kHz and detected with a photodiode and lock-in amplifier. The samples are maintained at 5 K in a liquid-helium cryostat. Because the lattice temperature is 5 K and the excitation energy is resonant with the exciton line, the carriers photoexcited in the narrow well should consist of a gas of cold excitons.

EXPERIMENTAL RESULTS

Characteristic transmission spectra for the samples and conditions in this study are presented in Fig. 1. The solid line spectra in (a) and (b) are the unperturbed, no-pump-pulse spectra. Figure 1(a) shows various time-delayed spectra for the pump resonant with the $n=1$ heavy-hole exciton in the *wide well* (WW1) with a photoexcited carrier density of 7.0×10^{9} cm^{-2}. Figure 1(b) presents similar spectra for the pump resonant with the $n=1$ heavy-hole exciton in the *narrow well* (NW1) with a photoexcited carrier density of 1.4×10^{10} cm^{-2}. Note that the narrow-well absorption is unperturbed when the pump is in the wide well, while there is absorption bleaching in both wells for the pump in the narrow well. This proves

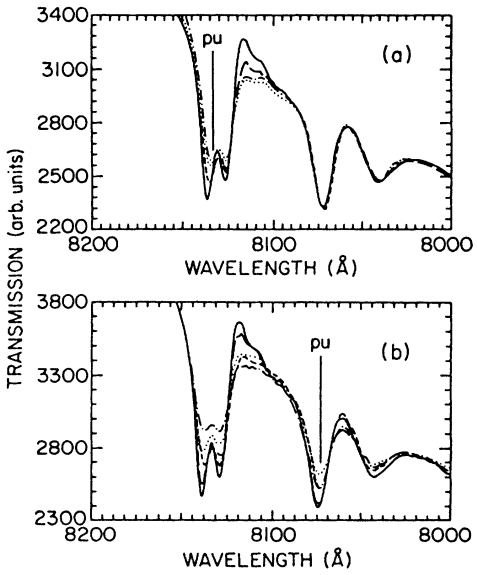

FIG. 1. Transmission spectra for the 30-Å-barrier sample. (a) Time evolution of the absorption spectra after photoexciting a carrier density of 7.0×10^{9} cm^{-2} with the excitation pulse in resonance with the *wide well* $n=1$ heavy-hole exciton: (——) no pump, (— —) 0 ps, (·····) 10 ps, (—·—·—·) 50 ps, and (---) 500 ps pump-probe delays. (b) Absorption spectra following an excitation pulse in resonance with the *narrow well* $n=1$ heavy-hole exciton and a photoexcited carrier density of 1.4×10^{10} cm^{-2}: (——) no pump, (— —) 15 ps, (·····) 25 ps, (—·—·—·) 110 ps, and (---) 510 ps pump-probe delays.

that with the sample temperature at 5 K and the carriers excited into the wide well, there is no reverse tunneling of carriers from the wide well to the narrow well.

cw photoluminescence data (not plotted) show that at 5 K with excitation into both wells, no luminescence is detected at the NW1 exciton for the 20-, 30-, and 35-Å-barrier samples. Some luminescence is seen at the NW1 exciton for the 40-Å-barrier sample, and still greater luminescence for the 300-Å-barrier sample. At elevated temperatures, on the other hand, the NW1 excitonic luminescence for the first three samples increases with temperature, whereas the NW1 luminescence for the 300-Å-barrier sample is steady to decreasing with increasing temperature. This establishes that carriers are able to tunnel into the narrow well from the wide well at elevated temperature in the narrow barrier samples, and that carriers tunnel from the narrow well into the lower energy wide well at 5 K. This tunneling process and its time dependence at 5 K is the subject of the remainder of this paper.

Figure 2 illustrates the dependence on pump-probe delay of the change in transmission of the probe pulse. Figure 2(a) presents two curves for the 40-Å-barrier sample; pump and probe in resonance with the WW1 exciton in the wide well (slow decay), and pump and probe in resonance with the NW1 exciton in the narrow well (more rapid decay). Both curves are measured at an initial carrier density of 7.0×10^{9} cm^{-2}. As we would expect, there is a rapid initial change in transmission corresponding to carriers populating the wells as the pump pulse is absorbed. Following this initial rise there is a steady decrease in transmission which is linear on this semilog plot. This linearity indicates that the relaxation process is exponential with a single time constant. From an exponential fit to these curves we deduce decay time constants of 755 and 180 ps for the wide and narrow wells,

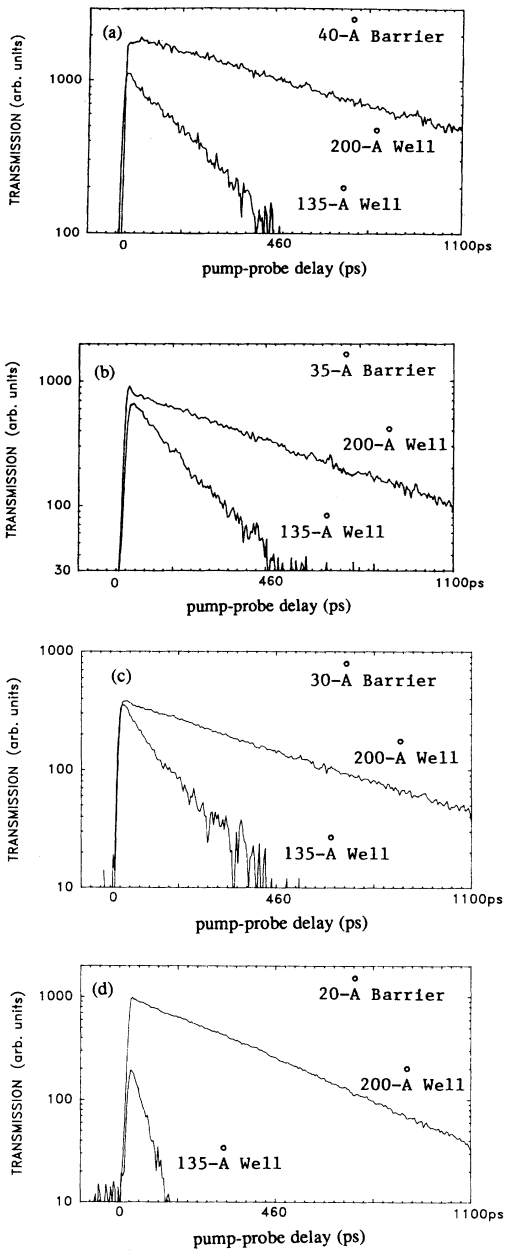

FIG. 2. Temporal evolution of absorption bleaching for an initial photoexcited density of 7.0×10^{9} cm^{-2}. Sample temperature is 5 K; both the pump and probe wavelengths are in resonance with the lowest energy excitonic transition for the well being measured. Data are plotted for samples with barrier width (a) 40 Å, (b) 35 Å, (c) 30 Å, (d) 20 Å. Lifetimes from single exponential fits to the data are presented in Table I.

TABLE I. Measured lifetimes (ps) for the $n=1$ heavy-hole exciton in the wide and narrow wells for an initial photoexcited carrier density of 7.0×10^9 cm^{-2} at a lattice temperature of 5 K. The table also presents estimated values for the narrow-well recombination time as well as the tunneling time that is derived, as discussed in the text.

Barrier width	300 Å	40 Å	35 Å	30 Å	20 Å
Measured lifetime					
Wide well τ_{expt} (ps)	580	755	615	510	340
Narrow well τ_{expt} (ps)	370	180	135	110	65
Estimated recomb. time					
Narrow well τ_R (ps)	390	510	415	345	230
Tunneling time τ_T (ps)		278	173	162	91

respectively. Figure 2(b) presents similar data for the 35-Å-barrier sample. Again we observe a rapid rise in transmission followed by simple exponential decay for each curve. Decay curves are shown for the 30- and 20-Å-barrier samples in Figs. 2(c) and 2(d), respectively. Measurements on the control sample with 300-Å barriers yield lifetimes of 580 and 370 ps for wide and narrow wells, respectively. The decay time constants for the narrow and wide wells of all five barrier widths are summarized in the first two rows of Table I. There is a variation of a factor of 2 in WW1 exciton lifetimes. The times appear to increase with increasing barrier thickness except for the shorter time found for the 300-Å-barrier sample. We cannot conclude that the trend is physically significant on the basis of these five samples and attribute the variation instead to variation in sample quality. The NW1 exciton lifetime is uniformly shorter than the corresponding WW1 exciton lifetime in each sample and varies by a factor of 6, increasing monotonically with increasing barrier thickness. In the next section we show how to normalize these times by the variation found in the WW1 exciton lifetime.

We have measured narrow-well lifetimes in each of the tunneling samples as a function of photoexcited carrier density. These measurements are illustrated in Figs. 3(a) and 3(b) for the 40- and 35-Å samples, respectively; the fitted lifetimes are summarized in Table II. The behavior in each figure is similar; the slope of the decay decreases with increasing carrier density. We note that in Fig. 3(b) there is a decrease in slope in each of the decay curves as the induced transmission falls below 10% of its maximum. We believe this change in slope is due to a slight dc shift in the detected signal that is most likely caused by leakage of the pump beam into the photodiode used to detect the probe.

TABLE II. Density dependence of carrier lifetime in the narrow well. Pump and probe wavelengths are tuned to the $n=1$ heavy-hole exciton in the narrow well, lattice temperature is 5 K, and lifetimes (ps) are from single exponential fits to the data shown in Fig. 3.

Barrier width: Carrier density (cm^{-2})	40 Å τ_{expt} (ps)	35 Å τ_{expt} (ps)
1.4×10^9	142	103
3.5×10^9	161	111
7.0×10^9	179	133
1.4×10^{10}	194	139
3.5×10^{10}	237	161
7.0×10^{10}	246	195

DERIVATION OF RATES

The lifetimes derived from the photoinduced absorption measurements in the preceding section are composite lifetimes due to several processes. Figure 4 illustrates the dominant processes contributing to the measured lifetimes. Carriers are initially excited into both wells through absorption of pump photons. The only relaxation channel available in the wide well is recombination, both radiative and nonradiative. Carriers excited into the narrow well can relax by tunneling into the wide well or

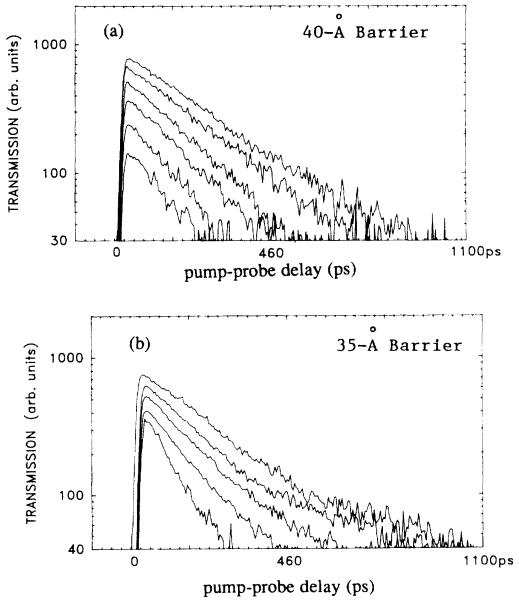

FIG. 3. Temporal evolution of absorption bleaching at the narrow-well excitonic transition for a series of initial carrier densities. Slope increases with decreasing density, indicating shorter lifetimes for lower densities. (a) shows data for the 40-Å-barrier sample; (b) shows data for the 35-Å-barrier sample. Lifetimes from single exponential fits to the data are presented in Table II.

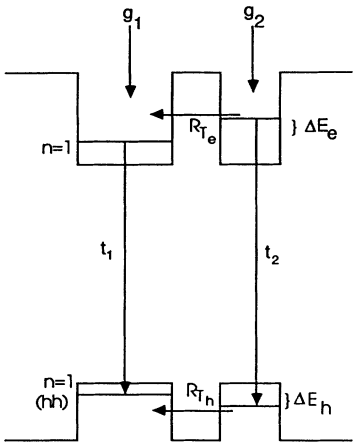

FIG. 4. Schematic representation of processes contributing to carrier population in each well for tunneling experiments. Photoexcitation of carriers is represented by g_1 and g_2, tunneling rates for electrons and holes are R_{T_e} and R_{T_h} respectively, and recombination lifetimes are t_1 and t_2 for the wide and narrow wells.

recombining within the narrow well. We may express the composite lifetime in the narrow well by adding these two relaxation rates:

$$\frac{1}{\tau_{\text{expt}}} = \frac{1}{\tau_T} + \frac{1}{\tau_R} . \tag{1}$$

In this expression τ_{expt} is the experimentally measured lifetime, τ_T is the tunneling time, and τ_R is the isolated well recombination time. To calculate the tunneling time from the experimental value we must estimate the recombination lifetime for the 135-Å well in each sample. A complication which arises in this analysis is that variation in sample quality is reflected in variation of lifetimes in the 200-Å wells, as shown in Table I. We cannot measure the decoupled NW1 exciton τ_R, but we do have the WW1 exciton τ_R for each sample. It has been shown that recombination times are inversely proportional to well width (because increased confinement produces greater electron-hole overlap).[18] We infer from this that the narrow-well τ_R should reflect the variation seen in the wide well, but scaled by $135/200=0.675$ times the wide-well lifetime. This argument is substantiated by the relatively good agreement this method produces between the estimated and the measured narrow-well recombination lifetime for the isolated narrow well in the 300-Å-barrier sample.

ANALYSIS

The process we are studying is a transition from the ground subband in the narrow well to the ground subband in the wide well. The confinement energies for the ground conduction subbands in the narrow and wide wells are 21 and 10 meV, respectively. An electron tunneling between these two levels must make a transition between two vertically displaced parabolic dispersion curves (representative of the dependence of energy on wave vector parallel to the interfaces). Thus a transition at constant energy requires a change in momentum, and conversely, a transition at constant momentum requires a change in energy. We conclude that tunneling in these samples must occur through nonresonant processes.

The available mechanisms which may contribute to tunneling are electron-electron scattering, phonon scattering, impurity scattering, and interface-roughness scattering. If electron-electron scattering were the dominant mechanism responsible for this "intersubband scattering" we would expect the tunneling rate to increase with increasing density. We have found just the opposite. As shown in Fig. 5 the tunneling rate is maximum at the lowest density of 1.4×10^{9} cm^{-2} and minimum at the highest density of 1.4×10^{11} cm^{-2}. Polar LO-phonon scattering of electrons is energetically forbidden for this transition since the energy separation is only 11 meV, whereas the LO-phonon energy in GaAs is 36 meV. Tunneling via acoustic-phonon scattering could satisfy energy and momentum conservation. Although we are unaware of a direct calculation of interwell transitions mediated by acoustic-phonon scattering, Ferreira and Bastard[19] have calculated intersubband scattering times within a single well in the range of 120–250 ps for well widths similar to those used in this study. By comparison we have measured tunneling times as fast as 55 ps in the 20-Å-barrier sample. We anticipate that *interwell* transitions through acoustic-phonon scattering will be much slower than intersubband transitions because of the decreased wave-function overlap for states in different wells, hence acoustic-phonon scattering is too slow to explain the short lifetimes measured in these samples.

IMPURITY SCATTERING

We are led to consider impurity and interface-roughness scattering as the primary mechanisms responsible for nonresonant tunneling in our experiments. Transition rates for both mechanisms will depend strongly on the concentration of scattering centers; however,

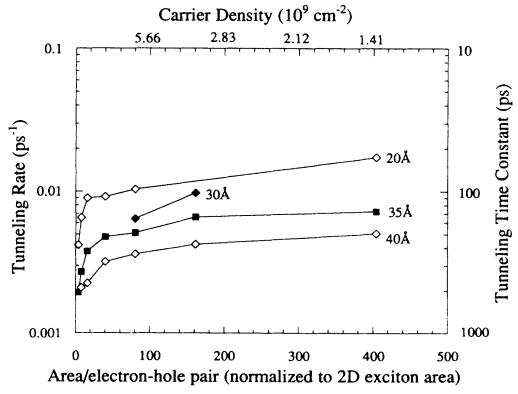

FIG. 5. Semilog plot of the density dependence of tunneling rates for each of four tunneling samples. Horizontal axis units are inverse of photoexcited electron-hole pair density normalized to the area of the 2D exciton assuming an exciton radius of 150 Å.

scattering due to interface defects is typically one to two orders of magnitude weaker than impurity scattering per scattering center. Ferreira and Bastard[19] calculated *interwell* scattering rates due to ionized-impurity scattering in an asymmetric double quantum well as a function of well width. Their interwell scattering time ranges from 8 ps to >1 ns depending on the proximity of a wide-well energy level to the narrow-well $n=1$ level. Allowing for differences between our well structure and the one considered by Ferreira and Bastard, we estimate that the corresponding time calculated for our structure should be 5 to 15 times longer than for theirs based on Eq. (2) below. Thus the 278-ps tunneling time deduced from our measurements for the 40-Å-barrier sample is compatible with impurity-assisted interwell scattering.

As with any extrinsic effect, an important signature of impurity scattering is its density dependence. As previously discussed, carriers photoexcited in the narrow well will consist of a gas excitons in the lowest subband. Since the exciton binding energy is slightly more than 7 meV,[20] while the separation of initial and final states ΔE is 11 meV, tunneling of either carrier to the wide well leaves little excess energy. Although the details of the tunneling process are not clear from the results of the present experiment, the excitons may remain bound through most of the tunneling process,[21] and may even tunnel as a single entity. With this in mind we have plotted in Fig. 5 the tunneling rate versus the area per photoexcited electron-hole pair normalized to the 2D-exciton area, assuming an exciton radius of 150 Å. There is a sharp decrease in the tunneling rate as the area per electron-hole pair falls below 10 exciton areas. Although a detailed dynamical calculation of the interaction between diffusion and tunneling is beyond the scope of this study, the measured density dependence is consistent with a model of excitons diffusing to, and then tunneling through, a limited number of "special" tunneling sites corresponding to impurities or interface fluctuations.

INTENSITY DEPENDENCE—SPECIAL SITES

A fixed limited number of special tunneling sites is a key feature of this model of impurity-assisted tunneling. At carrier densities which are low compared to the impurity concentration there will be a distribution of occupied and unoccupied sites due to the finite amount of time an exciton spends tunneling through a site. At densities much greater than the impurity concentration most tunneling sites will be occupied. If this site-blocking effect is a significant limiting factor, one would expect the tunneling rate to approach its maximum value as the ratio of excitons per tunneling site approaches unity. The MBE samples used in this study have an estimated volume impurity density of approximately 10^{15} cm^{-3}.[22] This corresponds to an areal density of 1.35×10^{9} cm^{-2} in a 135-Å-thick quantum well, or one impurity per 420 2D-exciton areas. The data in Fig. 5 suggest that the tunneling rates for the 20-, 35-, and 40-Å-barrier samples may be approaching a maximum tunneling rate at this density.

HOLE TUNNELING

Another effect which must be considered in this context is what is known as "effective mass filtering." This refers to the greater propensity for electrons to tunnel compared with holes due to the large difference in effective mass. In GaAs the electron effective mass $m^*=0.067m_e$ while for heavy holes $m^*=0.35m_e$, a ratio of 5.2:1. A simple expression for the quantum probability for barrier penetration assuming a square barrier is

$$P \propto \exp\left[\frac{-2L_b}{\hbar}\sqrt{2m^*(V-E)}\right], \tag{2}$$

where L_b is the thickness of the barrier, V is the barrier height, and E is the carrier energy. Using this expression we find that the ratio of tunneling probabilities for electrons versus holes ranges from ~20 for the 20-Å barrier to ~600 for the 40-Å barrier. This is but a rough calculation, yet it gives a reasonable estimate of the relative tunneling rates for different barrier widths. These different tunneling rates for electrons and holes can lead to a charge buildup between the two wells, producing an electric field which opposes tunneling by raising the barrier between the wells. Measurements of cw photoluminescence intensities in asymmetric $In_{1-x}Ga_xAs/InP$ coupled quantum wells have found that these charging effects start to become important only for barrier widths >40 Å, where the ratio of tunneling probabilities in that system is $\sim3.6\times10^{5}$, and at carrier densities larger than those used in these experiments.[4] We have calculated the induced potential assuming all of the electrons tunnel and none of the holes tunnel at the maximum carrier density used in our experiments. This is a maximum limit on the charging effect due to effective mass filtering. We find an upper limit of 7-meV potential difference between the two wells. In practice it will be much less than this estimate and hence much less than ΔE. Livescu *et al.*,[23] studying tunneling under applied electric fields through 57-Å $Al_{0.3}Ga_{07}As$ barriers, also found no evidence for space-charge buildup under similar excitation conditions. We conclude that space-charge effects due to effective mass filtering are not significant in the data presented here.

In summary, we have measured a strongly nonlinear density dependence of nonresonant tunneling rates between quantum wells in a structure where LO-phonon emission is not available to assist the tunneling process. Tunneling rates are highest at the lowest carrier density, and gradually decrease until a critical density of approximately one exciton per ten exciton areas, at which point the tunneling rate begins to decrease rapidly with increasing carrier density. These trends are independent of barrier width over the range we have measured. Although the evidence is not conclusive, this behavior is qualitatively consistent with a model of excitons diffusing to and tunneling through a finite number of extrinsic tunneling sites. Rigorous tests of this hypothesis should include theoretical calculations of the tunneling dynamics in conjunction with experiments designed to conclusively isolate extrinsic effects.

ACKNOWLEDGMENTS

We would like to thank Professor Y. Oono for his insight into the theoretical aspects of this problem, Professor Y. C. Chang for his assistance with band-structure calculations, M. Delaney and F. Slakey for many stimulating discussions, and C. O. Griffiths for his technical assistance in the laboratory. This work was supported by the National Science Foundation under Grant Nos. 86-12860 and 89-20538. The experimental work was performed in the Laser Facility of the Materials Research Laboratory at the University of Illinois in Urbana-Champaign.

---

*Present address: National Renewable Energy Laboratory (formerly Solar Energy Research Institute), 1617 Cole Blvd., Golden, CO 80401.

[1]R. Tsu and L. Esaki, Appl. Phys. Lett. **22**, 562 (1973).

[2]L. Esaki and R. Tsu, IBM J. Res. Develop. **14**, 61 (1970).

[3]For a review of transport studies, see F. Capasso, K. Mohammed, and A. Y. Cho, IEEE J. Quantum Electron. **QE-22**, 1853 (1986).

[4]R. Sauer, K. Thonke, and W. T. Tsang, Phys. Rev. Lett. **61**, 609 (1988).

[5]R. Sauer, T. D. Harris, and W. T. Tsang, Surf. Sci. **196**, 388 (1988).

[6]H. W. Liu, R. Ferreira, G. Bastard, C. Delelande, J. F. Palmier, and B. Etienne, Appl. Phys. Lett. **54**, 2082 (1989).

[7]T. B. Norris, N. Vodjidani, B. Vinter, C. Weisbuch, and B. A. Mourou, Phys. Rev. B **40**, 1392 (1989).

[8]D. Y. Oberli, J. Shah, T. C. Damen, C. W. Tu, T. Y. Chang, D. A. B. Miller, J. E. Henry, R. F. Kopf, N. Sauer, and A. E. DiGiovanni, Phys. Rev. B **40**, 3028 (1989).

[9]M. G. W. Alexander, M. Nido, W. W. Rühl, R. Sauer, K. Ploog, K. Köhler, and W. T. Tsang, Solid State Electron. **32**, 1621 (1989).

[10]F. Sasaki and Y. Masumoto, Phys. Rev. B **40**, 3996 (1989).

[11]M. G. W. Alexander, W. W. Rühle, R. Sauer, and W. T. Tsang, Appl. Phys. Lett. **55**, 885 (1989).

[12]M. Nido, M. G. W. Alexander, W. W. Rühle, T. Schweizer, and K. Köhler, Appl. Phys. Lett. **56**, 355 (1990).

[13]B. Deveaud, F. Clerot, A. Chomette, A. Regreny, R. Ferreira, G. Bastard, and B. Sermage, Europhys. Lett. **11**, 367 (1990).

[14]M. G. W. Alexander, M. Nido, W. W. Rühle, and K. Köhler, Phys. Rev. B **41**, 12 295 (1990).

[15]T. Matsusue, M. Tsuchiya, J. N. Schulman, and H. Sakaki, Phys. Rev. B **42**, 5719 (1990).

[16]K. Leo, J. Shah, J. P. Gordon, T. C. Damen, D. A. B. Miller, C. W. Tu, and J. E. Cunningham, Phys. Rev. B **42**, 7065 (1990).

[17]D. Y. Oberli, J. Shah, T. C. Damen, J. M. Kuo, J. E. Henry, J. Lary, and S. M. Goodnick, Appl. Phys. Lett. **56**, 1239 (1990).

[18]R. Höger, E. O. Göbel, J. Kuhl, and K. Ploog, in *Proceedings of the Seventeenth International Conference on the Physics of Semiconductors, San Francisco, 1984,* edited by J. D. Chadi and W. A. Harrison (Springer, New York, 1985), p. 551.

[19]R. Ferreira and G. Bastard, Phys. Rev. B **40**, 1074 (1989).

[20]R. L. Greene, K. K. Bajaj, and D. E. Phelps, Phys. Rev. B **29**, 1807 (1984).

[21]For a recent report of tunneling where excitons remain bound, see R. Ferreira, H. W. Lui, C. Delalande, G. Bastard, J. F. Palmier, and B. Etienne, Surf. Sci. **229**, 192 (1990).

[22]H. Morkoç (unpublished).

[23]G. Livescu, A. M. Fox, D. A. B. Miller, T. Sizer, W. H. Knox, A. C. Gossard, and J. H. English, Phys. Rev. Lett. **63**, 438 (1989).